Analysis of the role of Thermal Energy Storage in a Solar-Driven Polygeneration System for a dairy industry

Eduardo A. Pina[1], Luis M. Serra[1], M. Naveed Arif[1], Miguel A. Lozano[1] and Ana Lázaro[1]

[1]GITSE I3A, Department of Mechanical Engineering, Universidad de Zaragoza, Zaragoza (Spain)

Abstract

Solar-driven technologies have a great potential to meet the increasing energy demands in agri-food industrial sectors. Polygeneration systems can produce two or more outputs like electricity, cooling and heating. So, for agri-food industries, combining a polygeneration system with solar thermal energy can be a good approach for producing clean and efficient energy outputs, including heating, cooling and power. The technical, economic and environmental assessment of a proposed Solar Driven Polygeneration (SDP) system consisting of parabolic trough solar collectors coupled with a cogeneration Organic Rankine Cycle, auxiliary boiler, mechanical chiller, and thermal energy storage, covering the heating, cooling and electricity demands of a dairy industry located in Tauste, Zaragoza, Spain, has been studied. Several analyses encompassing: i) the assumption of selling or not electricity to the grid, ii) the study of the role of different thermal energy storages, iii) as well as sensitivity and robustness analyses, have been carried out for the proposed SDP system in order to assess the system performance at different operating conditions. The results showed that the proposed SDP system reached a solar fraction of 76% with a lower cost (close to 30%) and lower greenhouse gas emissions (close to 70%) as compared to the conventional energy supply system. Moreover, it was determined the effective contributions of the different thermal energy storages as well as the positive interaction with the electrical network, which was a "virtual" energy storage, in enhancing the SDP system's performance.

Keywords: Solar-driven Polygeneration System; Solar Thermal Energy; Optimization; Thermal Energy Storage; Agri-food Industries

1. Introduction

The Sixth Assessment Report of the Intergovernmental Panel on Climatic Change (IPPC) published in March 2023 confirms that: "Human activities, principally through emissions of greenhouse gases, have unequivocally caused global warming, with global surface temperature reaching 1.1°C above 1850–1900 in 2011–2020. Global greenhouse gas emissions have continued to increase, with unequal historical and ongoing contributions arising from unsustainable energy use, land use and land-use change, lifestyles and patterns of consumption and production across regions, between and within countries, and among individuals (high confidence)" (IPCC, 2023). Indeed, it is estimated that energy consumption accounts for more than two-thirds of total greenhouse gas emissions globally (IEA, 2021). For this reason, the energy sector is experiencing a major technological shift oriented towards a new model of clean production, encouraging the use of renewable energies on a large scale and an efficient management that attempt to minimize environmental burdens and improves the energy supply at affordable costs.

In this context of developing a new energy model mainly based on renewable energy sources pursuing to significantly reduce greenhouse gas (GHG) emissions, the European Union has committed to a legally binding target of reducing greenhouse gas emissions by at least 55% by 2030 compared to 1990 levels, increasing the share of renewable energy to 42.5%, and achieving full climate neutrality by 2050 (European Parliament and Council, 2023), and more than 70 countries, including China, Japan, South Korea and Canada, among others, have set a net-zero target (UN, 2025).

Discussing specific data on energy use, heating and cooling demands account for around half of global final energy consumption, of which 50% is consumed in industrial processes and 46% in residential and commercial

10.18086/swc.2025.06.02 Available at http://proceedings.ises.org

buildings (IRENA et al., 2020).

The reduction of this unsustainable energy usage to promote a low carbon economy hinges on energy efficiency. This implies that the energy supply must be based largely on renewable energy sources. At the same time, it needs to be flexible and fully integrated, exploiting the synergies and interactions between the different energy resources consumed and the conversion and storage technologies employed. In this respect, properly designed polygeneration systems have the proven capability of simultaneously producing different energy services with higher second law efficiency, lower economic cost, and reduced pollutant emissions, relative to the conventional energy supply (Serra et al., 2009).

Solar energy is suitable for several applications and is experiencing a rapid growth. Thus, globally, solar energy contributes 3.6 % of total electricity generation and accounts for 31% of all renewable energy sources. From 2010 to 2020, the installed capacity of solar PV increased from 40334 to 709674 MW, and the installed capacity of solar thermal increased from 1266 MW to 6479 MW (Pourasl et al., 2023).

Indeed, solar energy is a great option for driving polygeneration systems due to its many advantages: i) it is a free and inexhaustible energy resource, ii) it contributes to the diversification of the energy supply, iii) it reduces non-renewable primary energy consumption, iv) it has very low or zero greenhouse gas emissions during the operation of the system, and v) it presents a growing economic viability and wide social acceptance. Furthermore, a polygeneration system combined with solar energy can provide more cost-effective and environmentally friendly energy solutions for many applications than conventional energy sources (Bellos et al., 2022)

Given that solar energy is an intermittent resource and that its availability may or may not coincide with the consumer's energy demand, further benefits can be obtained by including energy storage devices, such as thermal energy storage (TES). This is a well-established and commercially available technology, whose application has been widely demonstrated in polygeneration systems for buildings (Pinto, 2021). The integration of TES can improve the efficiency, security and economic viability of polygeneration systems by storing excess energy and enabling a flexible use of the heat by decoupling production and consumption, allowing for example, the energy service production to be extended beyond sunlight hours, and promoting a better utilization of the other energy resources (Ferrari et al., 2024).

Thus, solar-driven polygeneration (SDP) systems are a promising technology for heating, cooling and electricity production in industries, particularly in agrifood industries, where energy is primarily used for various stages of food production, including processing, packaging, and refrigeration, which require significant amounts of heat, electricity, and cooling. Proper energy integration, considering the required operating temperatures of cost-efficient conversion technologies in SDP system can be an effective solution to cater the energy demand, as well as to enhance the utilization and consumption of renewable energy and assist the development of green and efficient distributed energy systems in agri-food industries (Mondal and De, 2022).

This study conducts a techno-economic and environmental analysis of a proposed SDP system for a dairy industry located in Tauste (41.9202º N & 1.2578º W and the elevation of 253 m), Zaragoza, Spain. The proposed system, covering the dairy plant's heating, cooling, and electricity demands, comprises parabolic trough solar collectors coupled with a cogeneration Organic Rankine Cycle, auxiliary boiler, mechanical chiller, and thermal energy storage. Several analyses encompassing: i) the assumption of selling or not electricity to the grid, ii) the study of the role of different thermal energy storages, iii) as well as sensitivity and robustness analyses, have been carried out for the proposed SDP system in order to assess the system performance at different operating conditions.

2. Energy demands and energy services of the dairy industry

The data for the analysis of the considered dairy industry were taken from two different sources: the annual energy demands were obtained from a Swiss dairy plant (Becker, 2012), and the hourly profiles of energy demands were developed according to a facility located in João Pessoa, Brazil (Correia et al., 2021). The energy services of the dairy industry, consisting of the pasteurization process, standardization, cleaning, space conditioning and building lighting, are covered with electricity, heating and cooling. Annual and peak demands are as follows: 2,328 MWh and 723 kW of electricity, 22,932 MWh and 7,124 kW of chilled water, and 11,376

MWh and 3,533 kW of hot water. The proposed SDP system must cover the hourly energy demands for the whole year. Figure 1 shows the monthly energy demands for cooling, heating and electricity. The dairy industry plant is open 16 hours per day on weekdays and 8 hours per day on weekends.

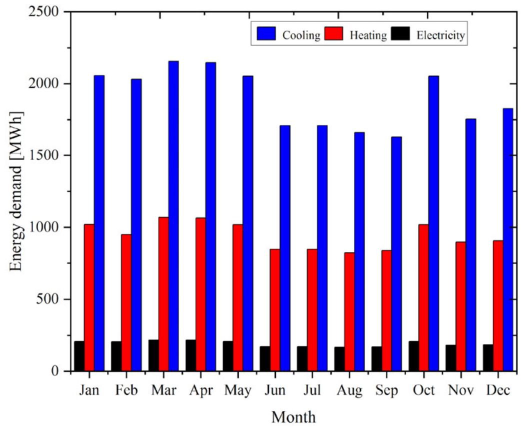

Figure 1: Monthly energy demand of cooling, heating and electricity of the dairy industry located in Tauste, Spain

Figure 2 shows the hourly energy demands of the studied dairy industry on weekdays in January (left) and July (right).

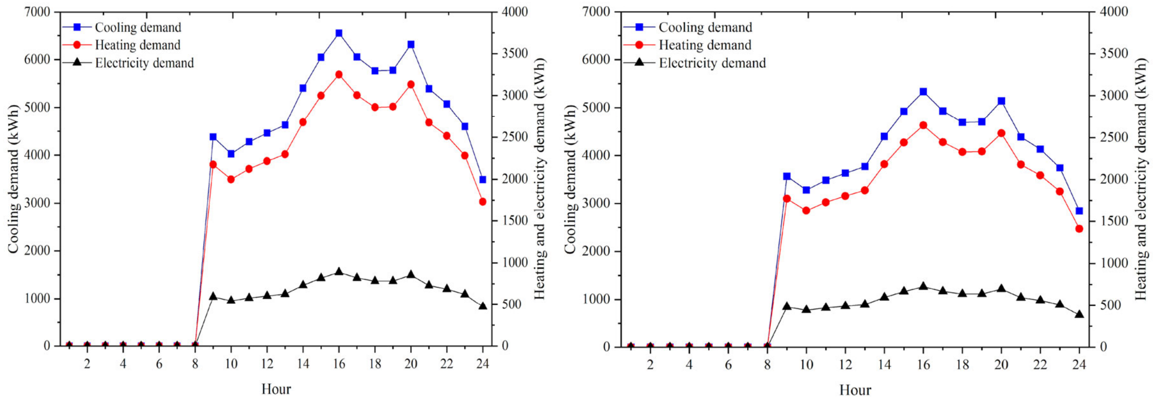

Figure 2: Hourly demands for weekdays in January (left) and July (right).

3. Description of the proposed solar-driven polygeneration system

Figure 3 represents the configuration of the proposed system designed to cover the dairy industry's electricity, cooling and heating demands. The proposed SDP consists of parabolic trough solar collectors (SKY) coupled with a cogeneration Organic Rankine Cycle (ORC), an auxiliary boiler (AB), a mechanical chiller (MC), and three different thermal energy storage units for the solar field (TESf), hot water tank (TESo) and chilled water tank (TESc). The solar collector SKY produces high-temperature heat at an average temperature of 320 °C to drive the ORC, which operates in cogeneration mode producing electricity (for the electricity demands and the MC to produce cooling) and waste heat (to cover the heating demand). Excess solar heat can be stored in the TESf unit or dissipated to the environment. Likewise, excess cogenerated heat from the ORC can be stored in TESo or dissipated. The TESc is installed after the MC to store chilled water. Es and Ep represent the electricity sold and purchased by the system. The AB provides heat to the system when there is insufficient heat from the ORC. Edem, Rdem and Qdem are the electricity, cooling and heating demands of the dairy plant, respectively.

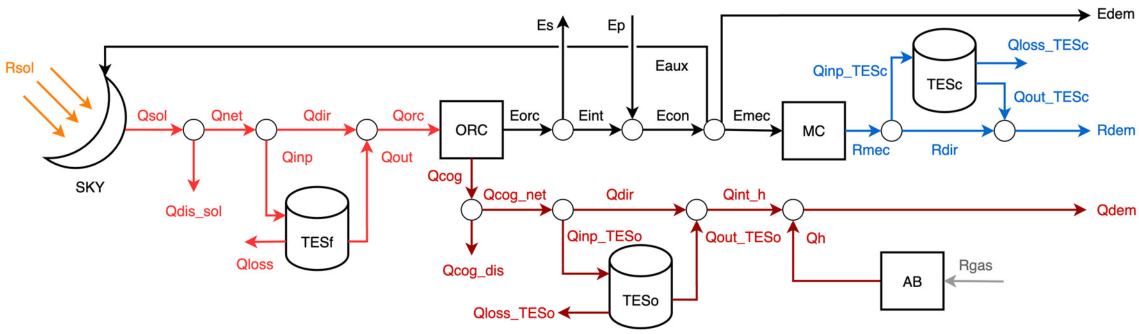

Figure 3: Proposed solar-driven polygeneration system for electricity, heating and cooling production for the dairy industry.

5.1. Technical features of the proposed Solar Driven Polygeneration (SDP) system

The technical specifications of the technologies considered in the analyzed SDP system, which correspond to commercial pieces of equipment, as well as the unit investment cost and the associated carbon emissions of the considered technologies, are shown in Table 1.

Table 1: Technical specifications of the considered technologies (Lozano et al., 2019; Pina, 2019; Gil, 2022; Glatzmaier, 2011; Wagner and Rubin, 2014; Guillen-Lambea et al., 2022).

Parabolic trough solar collectors (SKY)								
Model	Code	Aperture area, m^2	Receiver type	Optical efficiency, %	Thermal efficiency, %	Average Temperature, °C	Investment cost, €/m^2	Carbon emissions, $kgCO_2/m^2$
SkyTrough	SKY	39.2	Evacuated	76	72	320	400	126

Cogeneration Organic Rankine Cycle (ORC)									
Model	Code	Pn, kWr	CUq, kWq/kWr	PUq, kWq/kWe	Waste heat temp. °C	Tin, °C	Tout, °C	Investment cost, €/kW	Carbon emissions, $kgCO_2$/kWh
Rank @ HTC	ORC	968	5.31	4.21	90	300	240	2,100	0.176

Mechanical chiller (MC)								
Model	Code	$p_1 = p_2$ K^{-1}	Pn, kWr	c_1, K^{-1}	c_2, K^{-1}	CONMAZ, kWe/kWr	Investment cost, €/kWr	Carbon emissions, $kgCO_2$/kW
Centravac CHVV	MC	0	721	2.763E-3	0	0.181	140	72

Auxiliary boiler (AB)				
Model	Code	Power (kW)	Investment cost, €/kW	Carbon emissions, $kgCO_2$/kW
UT-L 30	AB	4,000	90	10

Thermal energy storages						
Manufacturer	Code	Tin, °C	Tout, °C	Energy loss factor h^{-1}	Investment cost, €/kWh	Carbon emissions, $kgCO_2$/kW
Idrogas	TESf	280	220	0.010	65	210
Eurotank	TESo	90	70	0.002	35	150
Eurotank	TESc	7	12	0.002	70	300

The model proposed by Kutscher et al. (2012) is applied for modelling the parabolic trough solar collectors SKY, which are arranged with the opening plane rotating along a horizontal north-south axis with a continuous east-west tracking that minimizes the angle of incidence:

$$\eta \equiv \frac{\dot{Q}_S}{A \cdot DNI \cdot \cos\theta} = -1.26 \cdot 10^{-6} x^3 + 3.02 \cdot 10^{-5} x^2 - 6.24 \cdot 10^{-4} x + 0.773, \quad x \equiv \frac{T_{avg} - T_a}{(DNI \cdot \cos\theta)^{0.33}} \qquad \text{(eq. 1)}$$

$$x = \frac{T_{avg} - T_a}{(DNI \cdot \cos\theta)^{0.33}} \qquad \text{(eq. 2)}$$

where T_{avg} represents the mean temperature of the heat transfer fluid within the collector (320 °C), while T_a represents the ambient temperature. DNI is the direct normal irradiance, and A is the collector aperture area. The term cos θ represents the cosine of the angle of incidence between the incoming solar rays and the normal (perpendicular) to the collector's surface (Kutscher et al., 2012). The solar production is calculated hour by hour throughout the year per m^2 of aperture area according to the ambient temperature, solar irradiance, and average working temperature of the solar collector. It is assumed that the solar field has an auxiliary electricity consumption equal to 1% of the solar heat produced.

The heat losses of TESo and TESc were calculated for cylindrical thermal storage tanks considering the wall and insulation thicknesses that correspond to the specific size of the storage tank and considering the specific climatic conditions of the study area.

For the mechanical chiller (MC), the heat rejected to the cooling water in the condenser is dissipated in cooling towers, and the cooling water temperature is determined according to environmental conditions. The specific nominal electricity consumption is calculated by eq. 3, where C_n is the nominal and C is the specific electric consumption, and T_r is the outlet temperature of the cooling water (Lozano et al., 2019):

$$\frac{C}{C_n} = 1 - c_1 \cdot (T - T_r) + c_2 \cdot (T - T_r)^2 \quad \text{(eq. 3)}$$

5.2. Energy resources of the proposed Solar Driven Polygeneration (SDP) system

The energy resources considered in this study are mainly solar energy and electricity from the grid, with the support of natural gas. The hourly ambient temperatures and solar irradiances were obtained from the software Meteonorm (Meteotest, 2015). An electricity tariff-scheme in Spain, consisting of 6 pricing periods has been considered whose prices range from 0.1708 €/kWh to 0.2485 €/kWh with an annual average price of 0.2104 €/kWh (Naturgy, 2024a). The system can sell electricity to the grid at 80% of the purchase price (r = 0.8). In order to evaluate the environmental benefits of the proposed SDP system, the hourly CO2eq emissions from the electricity grid have been considered as being the hourly values corresponding to the peninsular Spanish electricity production for the year 2016 (REE, 2024). The considered natural gas price is 0.11 €/kWh (Naturgy, 2024b), and the CO2eq emission factor corresponding to the natural gas in Spain is 0.202 kgCO2eq/kWh (MITECO, 2023).

4. Mathematical model

The pre-design of the SDP system was carried out through a mixed-integer linear programming (MILP) model developed in LINGO (Schrage, 2016). The optimization model determined the installed capacities of SKY, ORC, MC, and the three storage units, as well as the optimal operation, hour by hour, throughout the year. The installed capacity of AB has been fixed at 4,000 kW and has been sized to cover the heating demand when the solar system was not operative. The objective function minimizes the total annual cost, C_{tot}, which was calculated as the sum of the annual investment cost, C_{cap}, and the annual operation cost, C_{ope}, of the system.

$$Min\ C_{tot} = C_{cap} + C_{ope} \quad \text{(eq. 4)}$$

$$C_{cap} = (fom + fcr) \cdot \sum_t CINV(t) \cdot CAPINS(t) \quad \text{(eq. 5)}$$

$$C_{ope} = \sum_{h=1}^{8760} [P_{ep}(h) \cdot (E_p(h) - r \cdot E_s(h)) + P_g \cdot R_{gas}(h)] \quad \text{(eq. 6)}$$

where t represents the technology and h represents the hourly period. In eq. 5 an operational and maintenance factor, *fom*, of 0.015 yr^{-1} and a capital recovery factor, *fcr*, of 0.067 yr^{-1} were considered, based on an interest rate of 0.03 yr^{-1} and on an operational lifetime of 20 years. CINV represents the unit investment cost and CAPINS is the installed capacity of the conversion technology t. The calculation of the annual operation cost, C_{ope} (eq. 6), considers the electricity that is purchased and sold, as well as the natural gas that is consumed. P_{ep} and P_{gas} are the electricity and natural gas purchase prices, respectively.

The objective function is subject, among other restrictions, to capacity limits, production constraints, structural and operational restrictions and energy balances. For a detailed explanation of the model, the reader is referred to Pina (2019).

Once the optimization is solved, the annual solar fraction, SF (eq. 7), can be calculated as a function of the avoided electricity from the grid (E_p minus E_s) and heating demand covered by solar field relative to a conventional system in which all electricity and heating loads were supplied with electricity purchased from the grid and natural gas:

$$SF = \frac{[(E_{dem}+E_{mec})-(E_p-E_s)]+Q_{int}}{E_{mec}+E_{dem}+Q_{dem}} \quad \text{(eq. 7)}$$

where E_{mec} is the electricity required at a MC, E_{dem} is electricity demand of the system, Q_{int} is the heating demand covered by the solar field and Q_{dem} is the heating demand of the system.

In order to evaluate the environmental performance of the system model, the annual GHG (CO_{2tot}), which are the sum of the annual emissions corresponding to the pieces of equipment (CO_{2fix}) and to the operation (CO_{2ope}), are estimated:

$$CO_{2tot} = CO_{2fix} + CO_{2ope} \quad \text{(eq. 8)}$$

$$CO_{2fix} = \sum_t \frac{ZCO_2(t) \cdot CAPINS(t)}{nyr} \quad \text{(eq. 9)}$$

$$CO_{2ope} = [CO_{2ele}(h) \cdot (E_p(h) - E_s(h)) + CO_{2gas} \cdot R_{gas}(h)] \quad \text{(eq. 10)}$$

The CO_{2fix} emissions include the annual emissions associated with the installed pieces of equipment, which include ORC, TES, TESo. TESc AB, MC and SKY. The annual CO_{2ope} emissions consider the net emissions corresponding to the electricity purchase and sale to the grid as well as CO_2 emissions associated with the purchase of natural gas. ZCO_2 represents the unit embodied carbon emissions per unit of the considered characteristic dimension (see Table 1). CO_{2ele} is the hourly carbon emissions from the electricity in the Spanish grid, while CO_{2gas} is the emission factor of natural gas referred in section 2.

5. Results and discussion

The technical, economic, and environmental analysis of the proposed system SDP system depicted in Figure 3 was conducted. The SDP system was first evaluated under the assumptions of selling or not electricity to the grid. Further, the analysis was focused on the role of thermal energy storages TESo after the ORC and TESc after the MC, to evaluate the performance of the optimal SDP system in which electricity sale was allowed. Sensitivity and robustness analyses have also been carried out for this optimized SDP system to access the system performance at different operating conditions, as well as to assess system stability under changing external conditions.

5.1. Technoeconomic and environmental comparison of SDP cost optimal solution vs conventional system

The optimal results of the proposed SDP system shown in Figure 3 were compared in Table 2 with respect to a conventional system in which there is no solar energy and electricity is purchased from the grid to meet both electricity and cooling demands, while natural gas is purchased to meet the system's heating needs. In addition, Table 2 shows a comparison between different cost-optimal SDPs configurations oriented to analyze the effect of allowing or not the sale of electricity as well as the role of TES.

The results showed that the proposed optimal SDP system in which electricity sale was allowed achieved the highest solar fraction (76%) and was cost effective with respect to the conventional system, presenting 29% lower total annual costs and approximately 71% lower greenhouse gas emissions, thanks to a significant reduction in purchased natural gas (less than 80%) and electricity (less than 50%) as well as in electricity sold to the grid.

In the conventional system, the annual operation cost accounted for approximately 95% of the total annual cost. In absolute terms, the operation cost was more than 20 times higher than the annual capital cost. By contrast, in the proposed cost optimal SDP system in which electricity sale was allowed, the capital costs were close to 10 times higher than those of the conventional system. This is due to the installation of additional energy conversion technologies, including solar collectors, an ORC and TES units. The high investment required for the SDP system was offset by the substantial reduction in annual operation costs, which were approximately 72% lower than those of the conventional system, due to reduced reliance on grid electricity and natural gas.

The results also show that more than 80% of the annual heating demand in the proposed SDP system in which electricity sale was allowed was covered with cogenerated heat from the ORC. On the cooling side, the installed capacity of the mechanical chiller was reduced by 9% compared to the conventional system owing to the adoption of the chilled water tank TESc.

Table 2: Comparison of cost-optimal SDP systems vs. conventional system: analysis of the sale of electricity and the role of TESo and TESc

Results	Conventional system	Optimal SDP (electr. sale NOT allowed)	Optimal SDP (electr. sale allowed)	Optimal SDP without TESc (electr. sale allowed)	Optimal SDP without TESo (electr. sale allowed)	Optimal SDP without TESc and TESo (electr. sale allowed)
Annual solar fraction *SF*, %	-	67.0	***76.0***	76.0	73.7	73.8
Installed collector area, m^2	-	15,571	***18,662***	18,673	18,585	18,619
Installed capacity MC, kW	7,124	5,528	***6,473***	7,124	6,473	7,124
Installed capacity TESf, kWh	-	18,273	***18,335***	18,460	26,345	26,439
Installed capacity TESo, kWh	-	11,598	***15,551***	15,447	-	-
Installed capacity TESc, kWh	-	7,288	***867***	-	867	-
Installed capacity ORC, kW	-	903	***1,264***	1,264	1,148	1,151
Installed capacity AB, kW	4,000	4,000	***4,000***	4,000	4,000	4,000
E_p, MWh/yr	5,510	2,902	***2,607***	2,621	2,543	2,555
E_s, MWh/yr	-	-	***728***	744	629	649
R_{gas}, MWh/yr	11,866	2,820	***2,261***	2,260	2,635	2,629
Q_{cog}, MWh/yr	-	11,696	***16,122***	16,123	15,979	16,010
Q_h, MWh/yr	11,376	2,685	***2,153***	2,153	2,510	2,504
E_{orc}, MWh/yr	-	2,778	***3,829***	3,829	3,795	3,803
C_{cap}, €/yr	111,599	934,249	***1,083,777***	1,086,635	1,058,887	1,063,917
C_{ope}, €/yr	2,346,631	881,128	***661,326***	663,320	703,112	702,914
C_{tot}, €/yr	2,458,230	1,815,377	***1,745,103***	1,749,956	1,761,999	1,766,832
Emissions of CO_{2cap}, tonCO_2eq/yr	78	253	***266***	270	275	280
Emissions of CO_{2ope}, tonCO_2eq/yr	3,197	965	***687***	687	774	770
Emissions of CO_{2tot}, tonCO_2eq/yr	3,275	1,218	***953***	957	1,049	1,050

5.2 Analysis of the effect of selling electricity to the grid

Based on the results shown in Table 2, the optimal SDP system without electricity sale performed worse overall than the optimal SDP system with electricity sale. Prohibiting electricity sale to the grid decreased the annual solar fraction by about 12%, while the total annual cost and greenhouse gas emissions increased by approximately 4% and 28%, respectively. Furthermore, prohibiting electricity sale increased electricity and natural gas purchases by 11% and 25%, respectively.

A comparison of both previously referred optimal SDP systems showed that allowing electricity sale improved the affordability of electricity generation in the ORC with solar heat, as evidenced by a 20% larger solar field and a 40% higher ORC installed capacity. The auxiliary boiler in both systems (allowing electricity sale to the grid and prohibiting electricity sale) generated between 4–8 times less heat than the ORC.

It is worthy to mention that the hot water tank TESo was 34% larger in the SDP system in which electricity sale was permitted. As a result of the higher capacity for producing heat (higher solar field and higher ORC) and the higher size of the TESo, it was obtained that the annual heating demand covered with cogenerated heat from the ORC was higher in the optimal SDP in which electricity sale was permitted. Note that the size of the TESf (TES of the solar field) remained almost unchanged although the size of the solar field increased 20%, thanks to the bigger size of the ORC, and the higher capacity of the TESo and the exchange of electricity with the grid.

There were significant differences in TESc tank sizes between both previously referred optimal SDP systems. When electricity sale was permitted, the TESc capacity was relatively low (867 kWh); however, prohibiting electricity sale increased TESc capacity more than eightfold (7,288 kWh). Even though the proposed SDP systems introduced additional complexities, such as the possibility to exchange electricity with the grid and the production of cogenerated heat in the ORC, it was observed a clear relationship between the MC's cooling capacity and the size of the TESc storage, which varied inversely: the larger the storage capacity, the lower the required MC capacity. This is because the storage provided flexibility to the system to handle peak demands and to optimize operation strategies based on solar resource availability, electricity prices and energy demands.

Note that the optimal SDP system in which electricity sale was allowed had more flexibility and a greater utilization of the renewable resource than the optimal SDP system in which electricity sale was not permitted, mainly thanks to the interaction with the grid, which performed as a "virtual" energy storage, as well as with the positive interaction with the TES, which the role is analyzed in more detail in the next subsection.

5.3. Analysis of the role of hot water TESo and chilled water TESc (electricity sale allowed)

From the previous results, it was observed that the optimal SDP system with highest economic and environmental performance was that one in which electricity sale was permitted. It was thus decided to perform the analysis of the role of hot water TESo and chilled water TESc on that system. To do this analysis, first, TESc was excluded and the system was analyzed with the TESf of the solar field and TESo. Then, TESo was removed and the system was analyzed with TESf of the solar field and TESc. Finally, the system was analyzed considering only the TESf of the solar field (see Table 2).

The main results from Table 2 show that removing TESc has no impact on the solar fraction (SF) of the optimal SDP system with electricity sale, as the installed capacity of TESc is low (867 kWh). Therefore, the SF remains equal to the optimal SDP solution (76.0 %). However, when TESo is removed, the system experiences a lower SF of 73.7% because TESf has a larger capacity (26,345 kWh) and stores more heat throughout the year. Similarly, when both TESc and TESo are removed, the system's SF is reduced (76.8%), primarily due to the absence of TESo. The total annual cost of the system without TESc (1,749,956 €/yr) is marginally higher than the optimal SDP solution (1,745,103 €/yr) and also lower than the systems without TESo (1,761,999 €/yr). In terms of carbon emissions, the system without TESc generated 957 tons of CO2eq per year, slightly higher than those of the optimal SDP system due to increased emissions from the equipment. Without TESo, the system produced 1,049 tons of CO2eq per year, and when both TESc and TESo were removed, total emissions rose to 1,050 tons of CO2eq per year. In the latter cases, the increase in operational and mainly in fixed carbon emissions contributed to the overall rise in total emissions. An analysis of the annual breakdown of operational and fixed carbon emissions showed that the SDP system without TESc had lower emissions than the SDP system without TESo mainly associated to the operation. The increased emissions for the systems without TESo and without both TESo and TESc can be attributed to the emissions produced by the increase of size of the installed TESf and the larger difference between electricity purchased and sold.

When TESc is removed, the most significant change was that the MC capacity increased by 10%, remaining the installed capacities of the other pieces of equipment virtually unchanged with respect to the optimal SDP system. In the optimal SDP solution, the MC capacity (6,473 kW) was lower since TESc provided cooling during peak demand periods and the system purchased off-peak electricity from the grid and stored chilled water in TESc. The costs of the system without TESc slightly increased, both in terms of capital costs, due to the bigger MC installed, and in terms of operational costs, due to the increased purchase of electricity from the grid, although this increase of operational cost is partially compensated with the increased sale of electricity (note that the electricity produced in the ORC remains unchanged).

In contrast, the capacity of the MC in the system without TESo remains unchanged with respect to the optimal SDP system. The results further show that the installed capacity of the ORC (1,148 kW) in the systems without TESo is lower (9% lower) than in the other systems. Additionally, the gap between electricity purchased and sold and the amount of natural gas purchased is larger in systems without TESo, indicating higher net energy demand from the grid and from the gas network, and reduced reliance on solar energy.

The analyzed results indicate that TESo has a greater impact on the system. While TESc has a minimal effect on the overall performance of the SDP system, its inclusion can help lower total annual costs, as seen in both the optimal SDP system and the system without TESo. The simplest configuration, which includes only TESf at the solar field, has the highest total annual cost compared to the other systems. This indicates the effective contributions of both TESo and TESc in enhancing the SDP system's performance.

Finally, it is interesting to stress the connection among the TESf and TESo. Thus, when TESo is removed the size of installed TESf increases very significantly (close to 44%), even with a similar area of installed solar collectors. The reason is the need of matching the availability of the solar resource with the optimal production of the ORC, which in turn its installed capacity is also reduced, as previously referred.

5.4. Sensitivity analysis of the optimal SDP system (electricity sale allowed)

A sensitivity analysis of the optimal SDP system was performed by varying the purchase prices of electricity and natural gas. The sensitivity analysis on the electricity purchase price was performed by optimizing the whole system (size of pieces of equipment and operation) multiplying the electricity purchase price by a factor ranging from 0.5 (i.e., a 50% decrease) to 1.4 (i.e., a 40% increase). Figure 4 (left) shows a sharp increase in the annual solar fraction (SF) as electricity prices rise, due to an increase in the system's collector field area, as well as in the capacities of the solar field storage TESf and ORC. As a result, although not shown in the figure, the SDP system not only generated more electricity but also exported it more. Additionally, the capacity of hot water tank TESo also increased, while the capacity of chilled water tank TESc remained nearly constant, and both electricity and natural gas purchased by the SDP system decreased. As shown in Figure 4 (right), total annual cost of the system slightly decreased with increasing electricity prices. Despite the higher capital costs, annual operation cost decreased thanks to the revenues from electricity sales. There is also a significant reduction in the system's total annual carbon emissions as electricity prices decrease, because more energy was generated from the renewable sources.

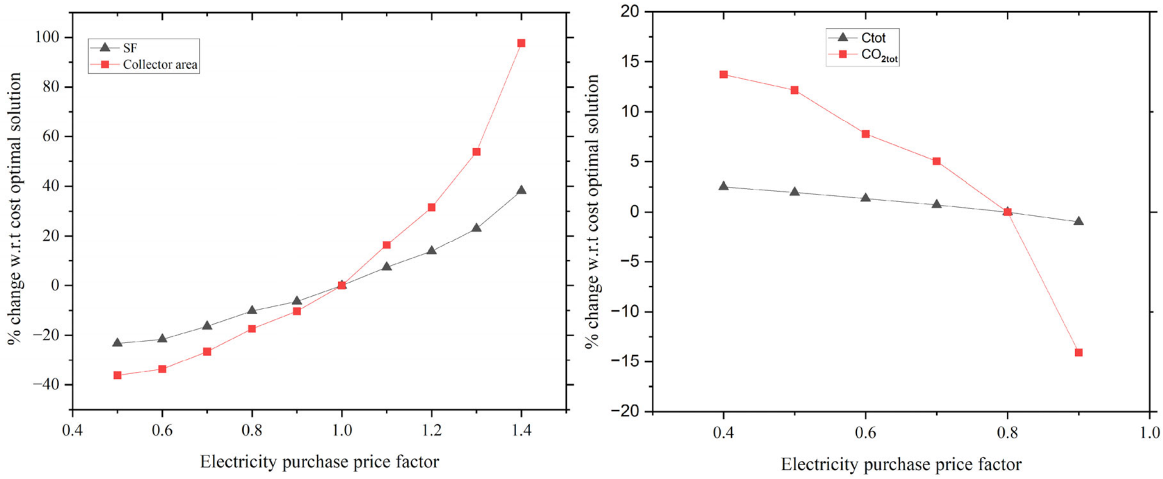

Figure 4: Variation in annual solar fraction (SF), collector area, total annual cost (Ctot) and greenhouse gas emissions (CO2tot) relative to the optimal SDP solution (electricity sale allowed) for different electricity purchase prices

A second sensitivity analysis was performed by varying the natural gas price factor, ranging from 0.5 (i.e., a 50% decrease) to 1.4 (i.e., a 40% increase). The results show an increase in the annual solar fraction and solar collector field area (Figure 5, left) with rising natural gas prices. Nevertheless, note that the impact is lower than in the sensitivity analysis in which the electricity price was varied. As the natural gas price increased, the optimal SDP system also sold more electricity to the grid and purchased less electricity and natural gas. Although the annual operation cost of the system decreased, it was not enough to offset the increase in capital cost, and the total annual cost of the optimal SDP system rose (Figure 5, right). Similarly to the previous sensitivity analysis, the total annual carbon emissions decreased with higher natural gas prices, because the system increased the share of renewable energy used to supply to the dairy industry.

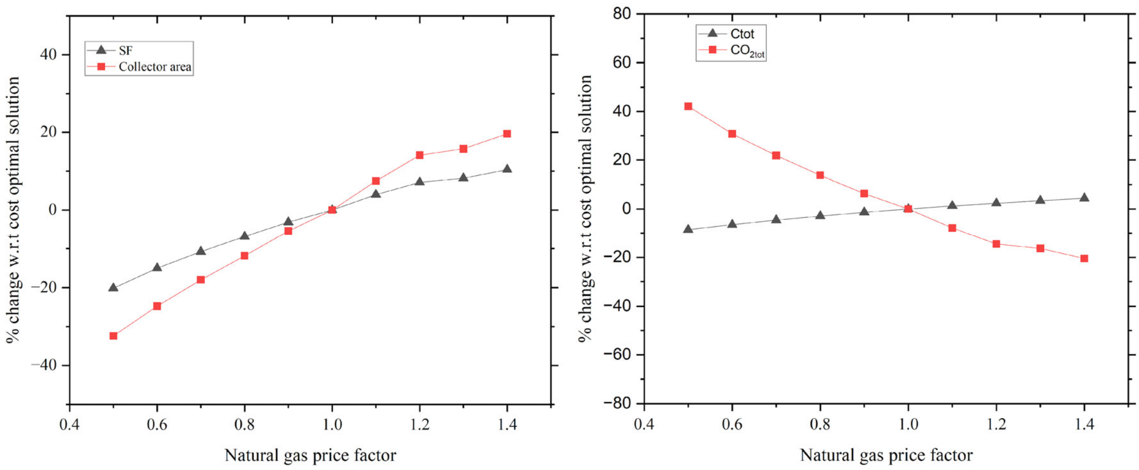

Figure 5: Variation in annual solar fraction (SF), collector area, total annual cost (Ctot) and greenhouse gas emissions (CO2tot) relative to the optimal SDP solution (electricity sale allowed) for different natural gas purchase prices

5.5. Robustness analysis of the SDP system (electricity sale allowed)

To assess the stability and reliability of the proposed optimal SDP system it was also performed two different robustness analyses. For this purpose, the system was first considered fixed, i.e. it was considered in this first robustness analysis that the system was already built and the installed capacities of the equipment were considered fixed and with the same size than those corresponding to the optimal SDP system with electricity sale. Therefore, in this first analysis it was only optimized the operation of the SDP system by varying the electricity and natural gas prices. Obviously operational costs increased when electricity and natural gas prices raised. The SF and carbon emissions remained almost constant when both the price of electricity or natural gas varied because the size of the technologies that include the solar collector were fixed. Interestingly, when the price of electricity increased the energy flows in TESf and TESo also increased because the system tried to store more energy reducing the heat dissipation. Nevertheless, when the price of natural gas increased the ORC increased the production of heat (as well as of electricity) in order to reduce the consumption of natural gas and the dependance on the AB. Additionally, the heat flows into the TESf decreased because the ORC directly utilized de solar heat to meet heating demands. When comparing the total cost of the analyzed fixed SDP system (with electricity sale and with the capacities of the pieces of equipment fixed) with respect to a conventional system, it is shown in Figure 6 that there is a significant saving in the case of the fixed SDP system when either electricity price or natural gas price or both experienced a variation, being higher the saving when the prices of energy resources are increased, with a sharper variation with the natural gas.

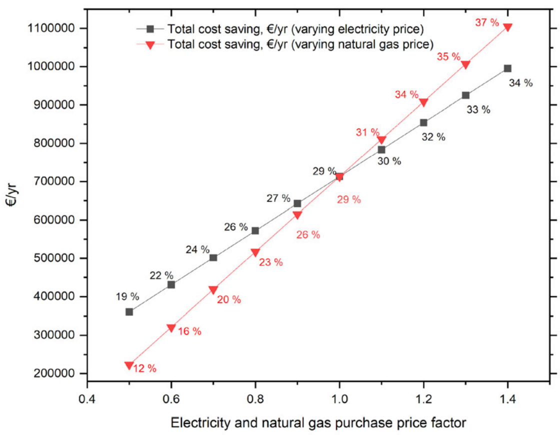

Figure 6: Total annual cost saving for a fixed SDP system as compared to a conventional system when the electricity and natural gas prices are varied

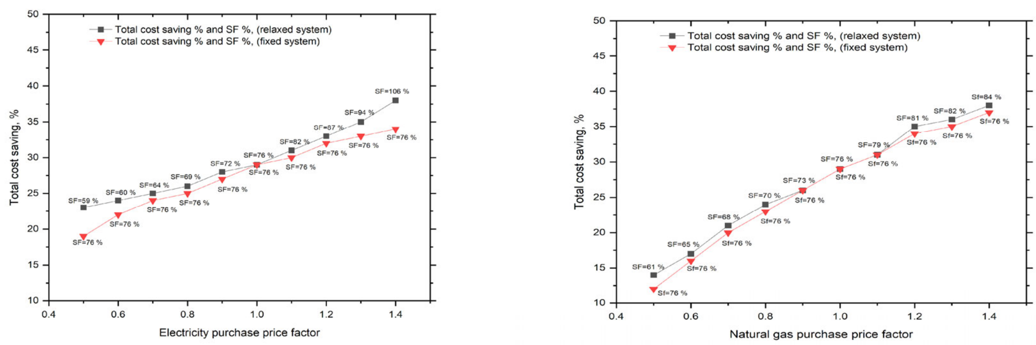

Figure 7: Total annual cost saving and solar fraction for a fixed SDP system and a "relaxed" SDP system with respect to a conventional system when the electricity (left) and natural gas (right) prices are varied

In a second robustness analysis the savings with respect to a conventional system were compared for the fixed SDP system with respect to an optimized SDP system, so called "relaxed system", in which both the sizing of the technologies as well as the operation were optimized for each different purchase price factor of electricity and natural gas. Figure 7 (left) shows that when the electricity price is varied, the total annual cost savings in the flexible system with respect to the conventional system is higher compared to savings achieved in the fixed system. This is because in a hypothetical flexible system, the capacities of the installed technologies are optimized for each price factor and the system selects the optimal sizes of the technologies to minimize the total annual cost when the price of electricity varies. On the other hand, in the fixed system the conversion technologies are already installed and the operation of the system is constrained to the fixed capacities. This fact also explains why the SF of the fixed SDP system remains constant at 76%, while for the relaxed SDP system, the SF varies. Nevertheless, the difference among savings achieved by both systems (the set of optimal SDP systems for each purchase cost and the proposed fixed SDP system) is not higher than 5%. Figure 7 (right) shows the comparison of “relaxed” SDP system and fixed SDP system when the natural gas price is varied, showing that in this case the difference among savings achieved by both systems is even not higher than 3%. These results show the resilience, robustness and flexibility of the proposed SDP system which is able of adapting its operation to significant variations of electricity and natural gas prices.

6. Conclusions

The technical, economic, and environmental feasibility of SDP systems applied to a dairy industry located in Tauste, Spain, has been evaluated by: i) analyzing the possibility of selling electricity to the grid, ii) studying the role of different thermal energy storage systems, and iii) performing sensitivity and robustness analyses to evaluate the system's performance under different operating conditions. The optimal configurations of the proposed SDP systems were predesigned based on a mixed-integer linear programming model developed in LINGO.

The optimization results showed that both the total annual cost and carbon emissions of all proposed SDP systems were lower than those of a conventional energy supply system in which energy demand was met by grid electricity and natural gas. The optimal SDP system with the highest economic and environmental performance was the one that included all thermal energy storage (TES) and allowed the sale of electricity, achieving a 29% reduction in annual costs and a 71% reduction in annual CO2eq emissions compared to the conventional system. In addition, this SDP system offered the greatest flexibility and greater use of renewable resources, mainly thanks to its interaction with the grid, which functioned as a “virtual” energy storage facility, as well as the positive and synergistic interaction with the three TES.

The resilience, robustness, and flexibility of the proposed SDP system were demonstrated through the sensitivity and robustness analyses, which showed that the proposed SDP system was most sensitive to variations in electricity prices. It was also demonstrated that the studied SDP system was capable of adapting its operation to significant variations in electricity and natural gas prices, with lower annual costs and CO2eq emissions than the conventional system.

7. Acknowledgments

This work has been partially funded by the Spanish State Research Agency (research projects PID2020-15500RB-I00 and PID2023-148958OB-C21), the Government of Aragon (Ref: T55-23R), and the European Regional Development Fund (ERDF).

8. References

Becker, H.C., 2012. Methodology and Thermo-Economic Optimization for Integration of Industrial Heat Pumps, ÉCOLE POLYTECHNIQUE FÉDÉRALE DE LAUSANNE, LAUSANNE, GENEVA.

Bellos, E., Said, Z., Lykas, P., Tzivanidis, C., 2022. A review of polygeneration systems with CO2 working fluid, Thermal Science and Engineering Progress. 34, 101435.

Correia, V.H.L., De Abreu, R.P., Carvalho, M., 2021. Robustness within the optimal economic polygeneration system for a dairy industry, Journal of Cleaner Production. 314, 127976.

European Parliament and Council, 2023, Directive (eu) 2023/2413 of the European parliament and of the council of 18 october 2023 on the promotion of energy from renewable sources (recast), 2023. [access 07 October 2025].

Ferrari, M.L., Gini, L., Di Barba, P., Mognaschi, M.E., Sieni, E., 2024. Multi-objective optimization of a polygeneration grid including thermal energy storage system, J. Energy Storage. 97, 112963.

Gil, L., 2022, Design and techno-economic evaluation of polygeneration systems for urban districts, carbon neutral, based on solar energy and thermal energy storage, MSc Thesis, Universidad de Zaragoza.

Glatzmaier, G., 2011. Developing a Cost Model and Methodology to Estimate Capital Costs for Thermal Energy Storage, Golden, CO (United States). DOI: 10.2172/1031953.

Guillén-Lambea, S., Pina, E.A., Serra, L.M., Lozano, M.A., Lazaro, A., 2022. Environmental assessment of medium-size solar organic Rankine Cycle cogeneration plants, Applied Thermal Engineering. 213, 118692.

IEA, 2021. Greenhouse Gas Emissions from Energy Data Explorer, IEA, Paris https://www.iea.org/data-and-statistics/data-tools/greenhouse-gas-emissions-from-energy-data-explorer. [access 07 October 2025].

IPCC, 2023. AR6 Sixth Assessment Report, UNEP https://www.ipcc.ch/report/sixth-assessment-report-cycle/ [access 07 October 2025].

IRENA, OECD/IEA, REN21, 2020. Renewable Energy Policies in a Time of Transition: Heating and Cooling. 2020 https://iea.blob.core.windows.net/assets/66a547ea-09bf-48fb-b7bb-6b94ef80b083/Renewable_Energy_Policies_in_a_Time_of_Transition_-_Heating_and_Cooling.pdf [access 07 October 2025].

Kutscher, C., Burkholder, F., Stynes, J.K., 2012. Generation of a Parabolic Trough Collector Efficiency Curve from Separate Measurements of Outdoor Optical Efficiency and Indoor Receiver Heat Loss, Journal of Solar Energy Engineering. 134, 1-6.

Lozano, M.A., Pina, E.A., Ramos, J.C., Serra, L.M., 2019. Thermal integration in polygeneration energy systems for buildings. CNIT11: XI National and II International Engineering Thermodynamics Congress, Albacete, Spain, 12–14 June.

METEOTEST, 2015. Meteonorm Global Meteorological Database. Version 7.

MITECO, 2023. Factores de emisión, registro de huella de carbono, compensación y proyectos de absorción de dióxido de carbono. Ministerio para la Transición Ecológica y el Reto Demográfico, Junio 2023.

Mondal, S., De, S., 2022. Polygeneration systems in industry. Polygeneration Systems, Elsevier.

Naturgy, 2024a. https://www.naturgy.es/negocios_y_autonomos/luz?vn=1581573559 [access July 24 2024].

Naturgy, 2024b. https://www.naturgy.es/negocios_y_autonomos/gas?vn=1581573559 [access July 24 2024].

Pina, E.A., 2019. Thermoeconomic and environmental synthesis and optimization of polygeneration systems supported with renewable energies and thermal energy storage applied to the residential-commercial sector, Ph.D. Thesis, Universidad de Zaragoza.

Pinto, E.S., 2021. Thermoeconomic and environmental optimization of polygeneration systems for small-scale residential buildings integrating thermal and electric energy storage, renewable energy and legal restrictions, Ph.D. Thesis, Universidad de Zaragoza.

Pourasl, H.H., Barenji, R.V., Khojastehnezhad, V.M., 2023. Solar energy status in the world: A comprehensive review, Energy Reports. 10, 3474–3493.

REE, 2024. Red Eléctrica Española. Emisiones de carbono de la red eléctrica. https://www.ree.es/es [access July 24 2024].

Serra, L., Lozano, M.A., Ramos, J.,Ensinas, A., Nebra, S.A., 2009. Polygeneration and efficient use of natural resources, Energy. 34(5), 575-586. DOI: 10.1016/j.energy.2008.08.013.

Schrage, L., 2016. Optimization modeling with LINGO, 6th Ed. Lindo Systems Inc.

UN, 2025. United Nations, Climate Action, Net Zero #Its Possible. https://www.un.org/en/climatechange/net-zero-coalition [access 07 October 2025].

Wagner, S.J., Rubin, E.S., 2014. Economic implications of thermal energy storage for concentrated solar thermal power, Renewable Energy. 61, 81–95.